RPE | Radiation Physics & Engineering
A Peer-Reviewed Journal
Published by K.N. Toosi University of Technology
http://rpe.kntu.ac.ir
Research Article

Radiation Physics and Engineering 2023; 4(4):35–42

Enhancing inertial confinement fusion with doped beryllium ablator layer in indirect drive scheme

Babak Khanbabaei*

School of Physics, Damghan University, P. O. Box 36716-41167, Damghan, Iran

HIGHLIGHTS

- ICF is a promising approach to generating practical energy through controlled fusion reactions.
- The efficiency of ICF is currently limited by the use of Be ablator material to contain the fuel.
- Researchers have proposed doping Be with various elements to enhance its performance as an ablator material.
- This study investigates the use of Na and Br dopants to improve the performance of Be ablator in indirect drive ICF.
- The results demonstrate that Na and Br dopants can improve the performance of Be ablator in indirect drive ICF.

ABSTRACT

Indirect drive inertial confinement fusion (ICF) holds promise for achieving practical energy generation through controlled fusion reactions. However, the efficiency of ICF is constrained by the Be ablator material used to contain the fuel. To overcome this limitation, researchers have proposed doping Be with various elements. In this study, we investigate the effects of Na and Br dopants, incorporated at concentrations of 4.86% and 2.1%, respectively, using a one-dimensional MULTI-IFE hydrodynamic code. This code serves as a numerical tool dedicated to analyzing Inertial Fusion Energy microcapsules, facilitating the examination of the Be ablator's performance in indirect drive ICF. Our results indicate that the addition of a beryllium layer doped with Na and Br significantly enhances the target gain, elevating it from the break-even value ($G \approx 1$) to approximately $G \approx 12$. Furthermore, we delve into the impact of these dopants on the plasma fuel conditions during the implosion, shedding light on the underlying physics of the system. These findings demonstrate that Na and Br doping in the Be ablator represents a viable approach for improving the efficiency of indirect drive ICF, potentially paving the way for the development of practical fusion energy systems.

KEYWORDS

Inertial confinement fusion
Indirect drive
Beryllium ablator
Doping

HISTORY

Received: 4 May 2023
Revised: 7 June 2023
Accepted: 13 June 2023
Published: Autumn 2023

1 Introduction

inertial confinement fusion (ICF), is a promising method for producing energy in an economical way (Lindl et al., 1992). This technique involves compressing a capsule containing a few milligrams of deuterium-tritium (DT) to high densities, around 1000 times the density of solids, using ion beams or laser drivers (Craxton et al., 2015; Logan et al., 2008). With the right conditions, the compression of the DT fuel leads to the formation of a central hot spot. Once formed, fusion reactions are initiated, and the self-heating caused by the alpha particles captured from these reactions far exceeds the cooling mechanisms, causing the hot spot to ignite (Atzeni and Meyer-ter Vehn, 2004; Pfalzner, 2006).

There are two principal ways to drive targets in ICF: direct drive and indirect drive (McCrory et al., 2008; Kawata, 2021). In direct drive ICF, laser or ion beams directly hit the target surface. In the indirect drive ICF method, the laser beams are first directed onto a small metal container called a hohlraum (Murakami and Meyer-ter Vehn, 1991). The hohlraum then emits x-rays, which are focused onto the fuel capsule containing DT. The fuel is then compressed and heated by the X-rays, leading to fusion. The main advantage of indirect drive ICF is that the hohlraum can be designed to produce a more uniform compression of the fuel capsule, resulting in more efficient fusion. Additionally, the hohlraum can be made from materials that can withstand higher temperatures and pressures than the fuel capsule, making it possi-

*Corresponding author: b.khanbabaei@du.ac.ir

https://doi.org/10.22034/rpe.2023.395904.1133
https://dorl.net/dor/20.1001.1.26456397.2023.4.4.5.5

ble to achieve higher fusion temperatures and pressures (McClarren et al., 2021).

One of the critical components of an indirect drive ICF target is the ablator material. Indirect drive capsules have traditionally been composed of plastic (CH), which has the advantage of being able to be filled with DT by diffusion and can be easily doped with higher Z material to achieve higher average opacity (Dittrich et al., 2014; Hinkel et al., 2016). However, CH ablators are highly sensitive to instability growth caused by roughness in the DT ice. Therefore, Beryllium (Be) capsules have been considered as an alternative to CH for the National Ignition Facility (NIF) laser due to their high strength, low atomic number, and good optical properties (Loomis et al., 2018; Zylstra et al., 2018). However, the ablation process still led to hydrodynamic instabilities that could degrade target performance (Kritcher et al., 2018; Kline et al., 2019).

Doping the ablator with a high Z material can help to mitigate these instabilities and improve target performance (Tikhonchuk, 2020). Additionally, a high Z dopant can be added to increase opacity, which helps to adjust the penetration of the radiation front into the ablator (Haan et al., 2004). In a rocket model, this separation of the fuel and unablated mass from the heated ablator is critical. Capsules can be optimized over a broad range of hohlraum temperatures by adjusting the concentration or thickness of the high Z dopant in the ablator.

In numerous research studies conducted at the National Ignition Facility (NIF), two primary categories of doped impurity compounds have been extensively employed concerning beryllium ablators (Lindl, 1995; Huang et al., 2012; McEachern and Alford, 1999; Landen et al., 2008). The first category entails beryllium ablators doped with copper, whereas the second category involves beryllium ablators doped with sodium (Na) and bromine (Br). The most effective impurity percentages for these doped materials have already been determined and subsequently validated through experimental trials at NIF. To illustrate, the addition of 4.86% Na and 2.1% Br has been proven to enhance the stability of the ablator, thereby reducing fuel mixture occurrence (Lindl et al., 2004). Consequently, in the present investigation, we adopt the identical composition of the doped beryllium layer utilized in previous researches.

Due to the immense cost and size of experimental facilities, as well as the complexity and difficulty of diagnostics, much of the research in the field of inertial fusion relies on numerical simulations (He and Zhang, 2007; Slutz et al., 2003). The paper utilizes a code called MULTI-IFE, which employs a one-dimensional spherical model incorporating the fundamental physical phenomena needed to simulate and investigate inertial fusion targets (Ramis and Meyer-ter Vehn, 2016). These phenomena include two-temperature hydrodynamics, laser light absorption, heat conduction, multigroup radiation transport, thermonuclear burn, and alpha-particle transport. MULTI-IFE can simulate the implosion of an inner capsule situated in a hohlraum and driven by a pulse of thermal radiation (Ramis et al., 1988, 2012). Therefore, using the MULTI-IFE hydrodynamic code, this study aims to determine the optimal thickness of Be ablator doped with 4.86% Na and 2.1% Br for typical capsule in indirect drive ICF. We investigate the effects of doping on critical physical parameters, such as temperature, pressure, density, etc. during ignition and burn.

2 Methods

The MULTI-IFE code has been used to simulate the implosion of inner capsule placed in a hohlraum and driven by a pulse of thermal radiation (X-rays), taken from reference (Lindl, 1995). So, our study does not consider the interaction of ion or laser drivers with hohlraum converters and the production of X-rays in high-Z enclosure (as shown in Fig. 1-a). Here, we assume that the capsule can be treated as hydrodynamically isolated (i.e., ignoring any interaction with the plasma of hohlraum) and submitted to uniform and known isotropic thermal radiation. Figure 1b and Fig 1-c show the scheme of the target sector used, similar to reference (Lindl, 1995) and this research. The targets are consisting of a hollow shell capsule with an ablation layer and a cryogenic DT fuel layer with a central cavity (containing DT vapor). Additional information can be seen in Table 1.

The target used in this research has a similar structure to the target introduced in Table 1 and only the certain thickness of the inside part of the Be layer is doped with 4.86% Na and 2.1% Br. This target is symmetrically irradiated by a pulse of thermal radiation. The time variation of radiation temperature (temporal shape of Tr(t)) is shown in Fig. 2.

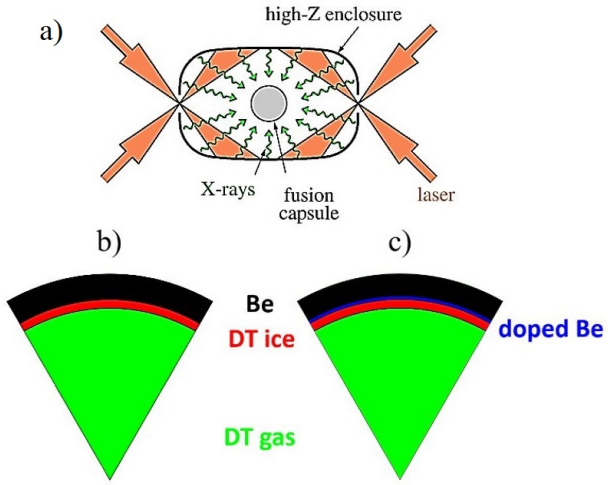

Figure 1: a) Typical hohlraum configuration. Laser beams heat the inner surface of a cylindrical high-Z casing (horizontal axis), and secondary X-rays drive the spherical fusion capsule. b) Scheme of the capsule with Be ablator c) Scheme of the capsule with doped Be ablator

Table 1: Target geometry used in Reference (Lindl, 1995).

Shell	Thickness (μm)	Mass (mg)	Number of cells
DT- vapor	980.0	≈ 0	40
DT-ice	50.0	0.14	100
Be- ablator	146.5	4.17	250

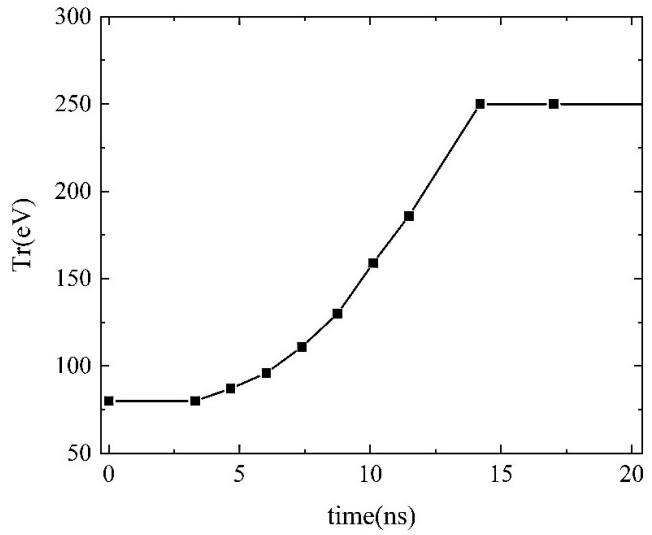

Figure 2: Time evolution of the temperature of the incident thermal radiation on capsule in hohlraum.

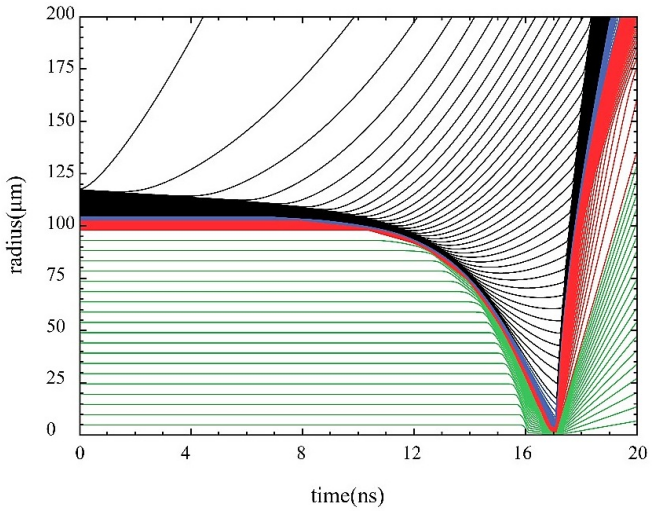

Figure 3: Implosion diagram of the capsule with doped Be ablator (Fig. 1-c).

Symmetrical and uniform radiation of X-rays causes an implosion of the shell of the target. Figure 3 presents a flow diagram visualizing the implosion process. To simulate the implosion, the target sphere was divided radially into 390 mass cells, and the trajectories of specific cell interfaces were recorded on the radius-time plane. This presentation is the natural one for the results of hydrodynamic computations performed in the Lagrangian approach. To ensure accurate simulations and avoid unphysical discontinuities, a non-uniform distribution of cell masses was employed in the target shell. Specifically, a larger number of cells were chosen, with denser cell populations in areas requiring finer resolutions. This is depicted in Fig. 3, where the trajectories of the selected cell interfaces appear as a densely packed filled area. Additionally, its worth noting that cell masses vary smoothly with the radius. Figure 3 demonstrates that X-radiation heats cells located on the outer surface of the capsule, causing them to expand, vaporize, and ionize. The heated cells interfaces are observed peeling off from the surface and ablating outward. Due to momentum conservation, the non-ablated inner portion of the capsule moves inward as a result of the ablation pressure. Increasing the x-radiation temperature in later times causes acceleration of the internal layers. The imploded layers reach the center of the capsule at about 16 ns, it hits the center and comes to rest. At this time the fuel stagnates and ignition occurs in the central hot spot. A burning wave is then running outwards, igniting the whole fuel, which expands rapidly as is clearly shown in Fig. 3.

The optimal thickness of the ablator and doped layer depends on the temperature and power of the X-radiation produced by the interaction of the driver beam with hohlraum converters. This optimal thickness is determined by physical parameters such as X-radiation absorption efficiency, loss radiation, thermal conduction of electrons, and ablation efficiency. Figure 4 shows the changes in important target parameters including a) fusion energy b) fuel burning fraction c) maximum ion and electron temperatures and d) maximum density for different thicknesses of the doped ablator layer. As can be seen, all these parameters have their maximum value in the approximate thickness of 18.5 μm.

One-dimensional simulations are highly idealized, because they impose spherical symmetry. Two-dimensional simulations show that even small irradiation nonuniformities cause large implosion asymmetries. Also, hydrodynamic instabilities cause important limitations in the design of ICF targets. Because plasma disturbances have a major impact on the formation and shape of the hot spot. One-dimensional hydrodynamic codes are not able to calculate such instabilities directly, because at least two dimensions are needed to calculate such instabilities. Control parameters are used to ensure the accuracy of one-dimensional codes. One of the most important of them is the in-flight aspect ratio (IFAR), which is defined as the ratio of the mean radius of the peak density of the shell to the overall thickness of the shell (Yamanaka, 1999). The IFAR for an implosion is usually evaluated when the shell has moved roughly a third of its radius. and calculate as follow:

$$\mathrm{IFAR} = \frac{R_{2/3}}{\Delta R_{2/3}} \tag{1}$$

According to research, it has been determined that a value of 30 for IFAR is the threshold beyond which the shell is susceptible to breaking apart during the acceleration phase of the implosion. Therefore, maintaining the IFAR below 30 is crucial for the success of the implosion. Achieving this requires careful consideration of the initial shell thickness and driver while ensuring the high velocity necessary for ignition later in the implosion is maintained. Another key design parameter is the convergence ratio, defined as the ratio of the initial inner radius of the shell to its final radius at peak compression with alpha-particle deposition turned off (Rosen, 1999). The convergence ratio places a constraint on the drive uniformity to ensure that all parts of the shell will converge at the center and form a spherically igniting hot spot. Additionally, the convergence ratio is related to the growth of hydrodynamic

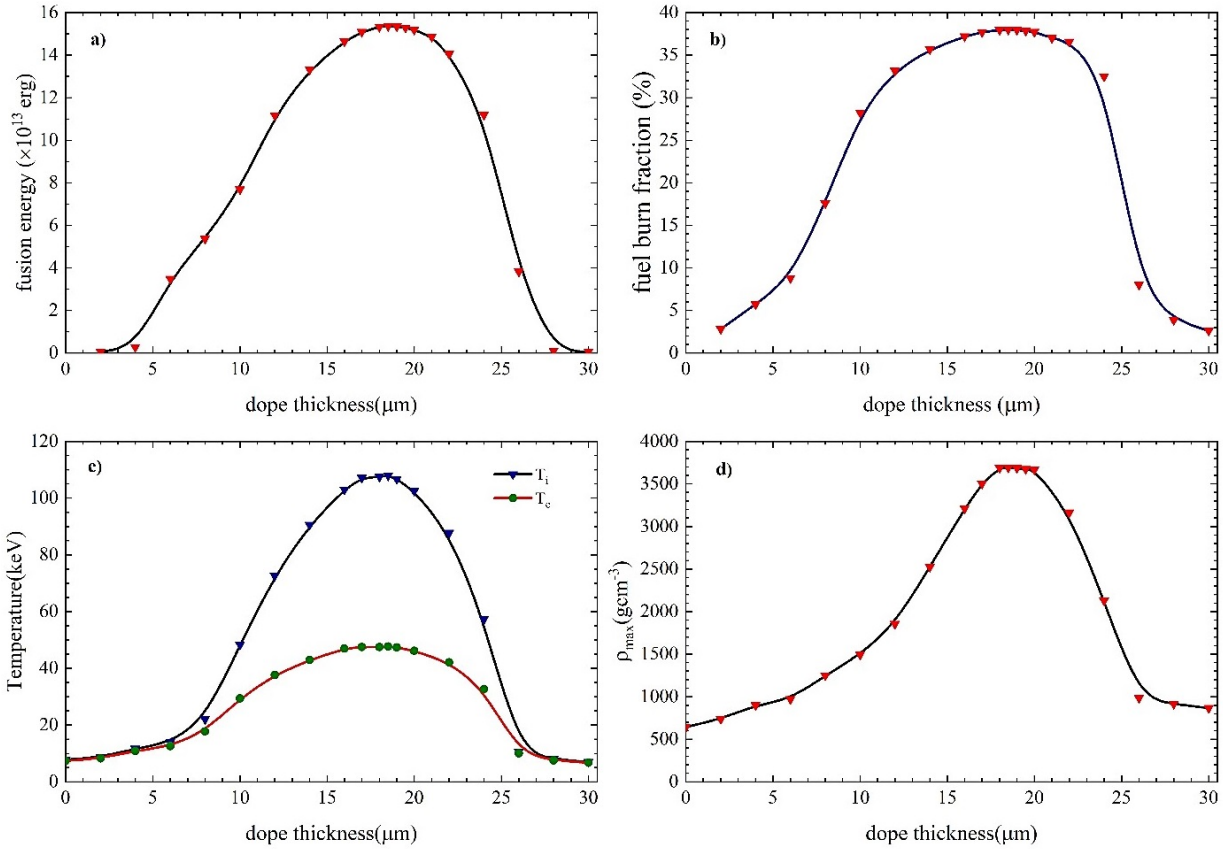

Figure 4: a) fusion energy b) fuel burn fraction c) maximum fuel ion and electron temperature d) maximum fuel density versus doped thickness in Be ablator.

instability during the deceleration phase of the implosion, which can hinder or prevent ignition. High convergence ratio designs (small hot spots) have a higher risk of failure, and it is generally recommended that the convergence ratio should not exceed 30 (Rosen, 1999).

2.1 Results and discussion

Table 2 illustrates the geometry specifications and mass of the layers utilized in the target of this study. Now, we examine the ablation of the target with Be ablator layer and then compare the effective physical parameters in ablation and ignition with the target containing the doped-Be ablator layer.

The ablative implosion of the shell is illustrated in Fig. 5, showing sequences of Lagrangian cell profiles of the ion temperature, mass density, and pressure during the stages of shell inward acceleration (13 ns and 15 ns), just 0.1 ns after rebounce of the first shock at the center (16.09 ns) and about the time of fuel ignition (16.99 ns). The density profiles in Figure 5c clearly show the inward motion of the compressed shell, driven by the pressure (Fig. 5-c) exerted onto the shell surface. When the imploding shock wave has reached the center (at about 16.09 ns) the inner gas is heated to a temperature exceeding 3 keV. At time 16.99 ns, peak pressure exceeds 300 Gbar, that is, more than 1000 times larger than the peak, and the temperature of the ions reach the ignition temperature (about 10 keV).

Figure 6 shows the radial profile of shell velocity during the time of implosion at time $t = 15.5$ ns for targets with 18.5 μm doped-Be and without doped-Be ablator layer. The ablated plasma expands with velocities exceeding 2×10^7 cm.s^{-1}, while the dense shell and the inner gas reached by the shock implode with a velocity of about 2.5×10^7 cm.s^{-1}.

Figure 7 shows the final stages of implosion, stagnation, and ignition of the target with a doped ablation layer in the time interval of 15 to 18 ns. The flow chart shows that at time $t = 16.09$ ns this shock reaches the target center and is reflected. The gas behind the reflected shock stagnates, as evidenced by the nearly horizontal trajectories in Fig. 7. When, at $t = 16.6$ ns, the reflected shock hits the inner surface of the dense shell, the shell starts decelerating. In the time interval between 16.09 to 16.99 ns, the kinetic energy of the shell is converted into internal energy, and the density increases. Then a hot spot is formed in the center, ignition started in the fuel and finally, the fuel ignited.

Table 2: Target geometry used in this research.

Shell	Thickness (μm)	Mass (mg)	Number of cells
DT- vapor	980.0	≈ 0	40
DT-ice	50.0	0.14	100
Doped Be- ablator	18.5	1.76	37
Be- ablator	128.0	3.71	256

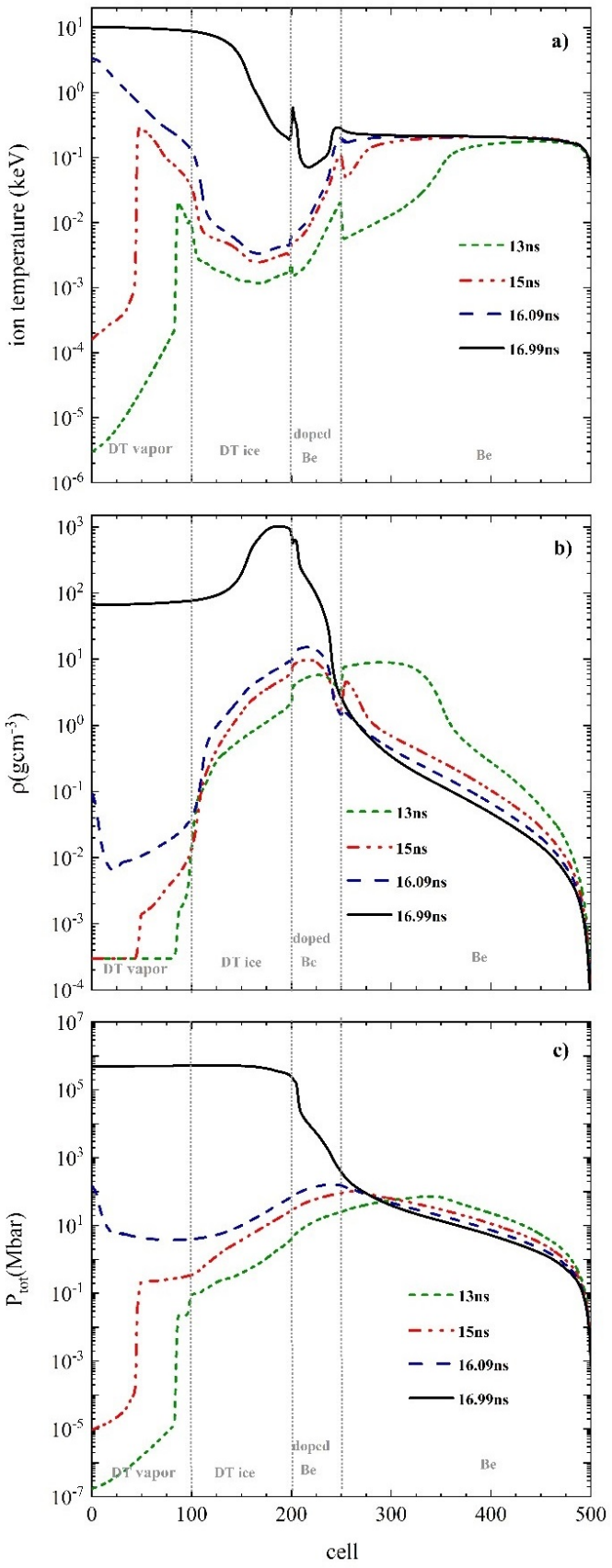

Figure 5: Sequences of Lagrangian cell profiles of (a) ion temperature, (b) density, and (c) pressure during the stages of shell inward acceleration (13 ns and 15 ns), just 0.1 ns after rebounce of the first shock at the center (16.09 ns) and about the time of fuel ignition (16.99 ns).

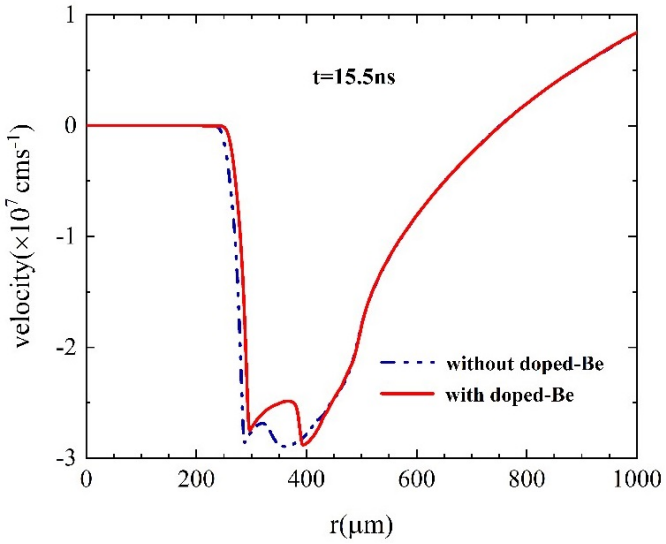

Figure 6: Fluid velocity versus radius at the approximate final implosion time (15.5 ns) with and without doped-Be ablator layer.

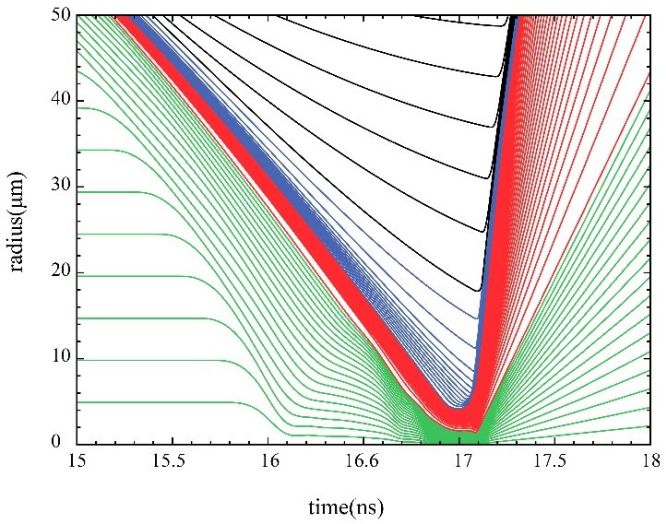

Figure 7: Enlarged view of the flow chart of the late stage of implosion, stagnation, and burn, in the time interval between 15 to 18 ns. The flow chart shows selected Lagrangian lines in the DT gas region (green lines) and the boundaries of the initial DT ice layer (red lines). The blue and the black curves represent the doped-Be and Be ablator layers respectively.

The time evolution of the total fuel confinement parameter (ρR) with and without the doped ablator layer is showen in Fig. 8. As depicted in the figure, the introduction of a doped layer leads to a delay of approximately 50 picoseconds in the formation time of the maximum confinement parameter. This delay can be attributed to the slightly heavier mass of the ablator layer. However, the maximum confinement parameter of the fuel with the doped ablator layer increases by approximately 6% in comparison to the fuel without an ablator layer. Consequently, a more efficient hot spot is formed, and the conditions for the fusion reaction are facilitated.

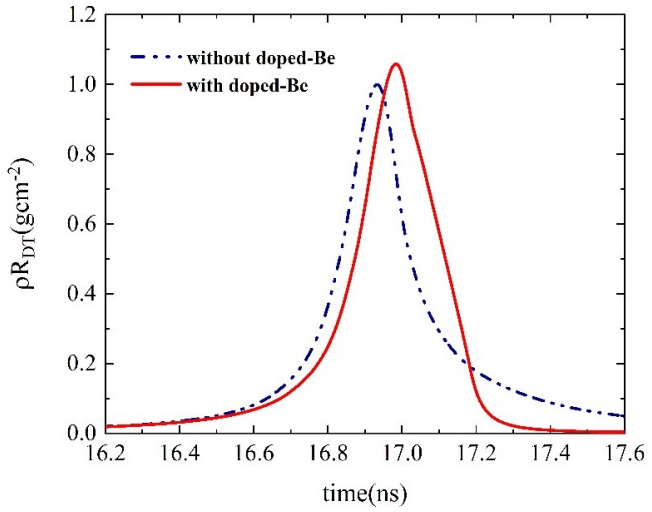

Figure 8: Time evolution of the mass averaged ion density in the fuel region with and without doped ablator.

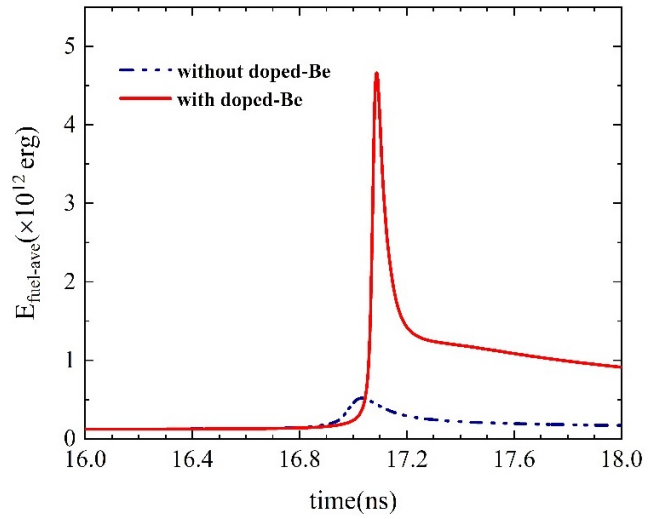

Figure 9: Time evolution of the fuel's internal energy in a late stage of implosion, stagnation, and burn.

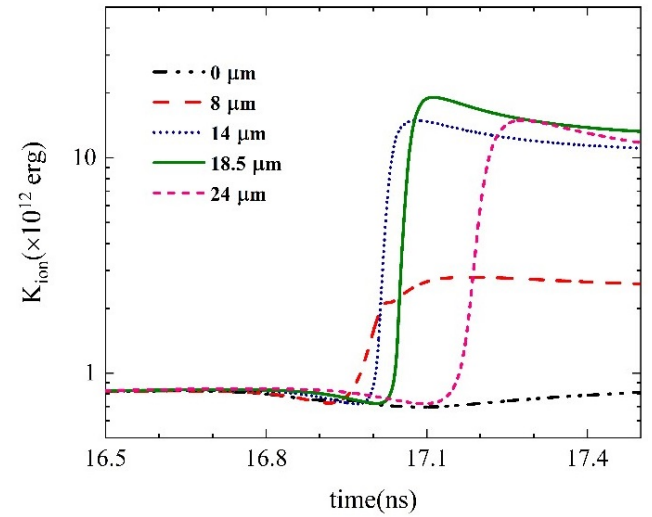

Figure 10: Time evolution of the fuel kinetic energy in a late stage of implosion, stagnation, and burn for different doped-Be thickness ablators.

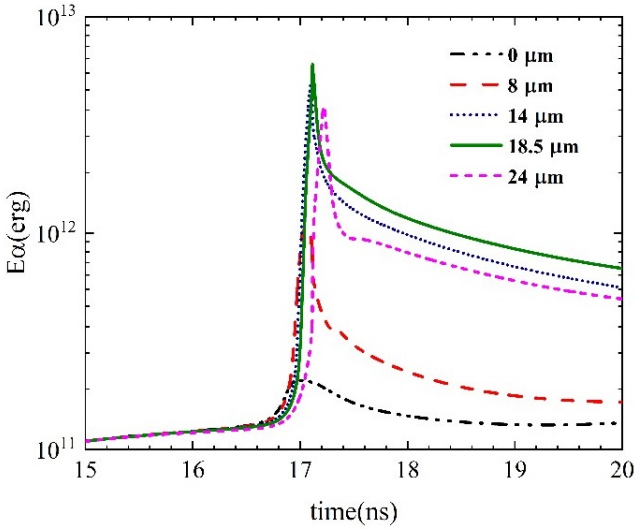

Figure 11: Time evolution of the fuel kinetic energy in a late stage of implosion, stagnation, and burn for different doped-Be thickness ablators.

Figure 9 illustrates the variation in fuel internal energy during the late stages of implosion, stagnation, and burn for targets with an 18.5 μm-thick Be-doped ablator layer and targets without a doped layer. The results show a significant increase in fuel internal energy in the target with the doped Be ablator layer compared to the undoped ablator layer. This increase in internal energy is attributed to the reflection of loss radiations generated during fuel burning by the doped layer. This increase in internal energy also translates to a higher hot-spot temperature, which improves ignition conditions compared to the undoped capsule.

Figure 10 displays the average changes in kinetic energy during the late stages of implosion, stagnation, and burn. To enable a comparison, these changes were determined for targets with doped layers of varying thicknesses. As the thickness of the doped layer increases, hot-spot formation is observed to occur at a later time. Specifically, in the target with a dope thickness of 24 μm, the hot spot formation time is approximately 0.3 ns later than in the fuel with an 18 μm doped layer. This delay can be attributed to the increased mass of the ablator caused by the thicker doped layer in the capsules. As the same driver power and energy are applied to accelerate the targets, hot spot formation time is consequently delayed. Moreover, increasing the thickness of the doped layer up to 18.5 μm causes the energy of the fuel ions to increase. The doped layer in the fuel has the capability to reflect the losses in radiation produced during fuel burning back into the fuel, leading to an increase in the hot-spot temperature with the increase in the doped layer thickness. However, further increasing the thickness of the doped layer causes the temperature of the hot spot to decrease, ultimately leading to a reduction in the energy of the fuel ions. This reduction is due to the constant intensity and driver power applied to the targets.

Figure 11 illustrates the energy distribution of alpha particles generated from the DT fusion reaction during fuel ignition time. It is observed that an increase in the

thickness of the doped layer up to 18.5 μm results in an increase in the energy of the produced alpha particles. As previously mentioned, during the DT burning process, fuel with a doped layer has the ability to reflect and partially confine loss radiations into the fuel, leading to an increase in the temperature of the hot-spot. As the thickness of the doped layer is further increased, the constant intensity and power of the driver lead to a reduction in the temperature of the hot-spot, ultimately resulting in a decrease in the energy of the produced alpha particles.

3 Conclusions

In conclusion, the use of a doped Be ablator layer in an indirect drive (hohlraum) inertial confinement fusion has shown to be a promising technique for improving fusion performance. Through a series of simulations, we have demonstrated that doping the Be ablator. layer with elements such as germanium, silicon, and carbon can significantly enhance the ablator's hydrodynamic stability, which ultimately leads to increased fusion yield. The improved stability arises from a combination of reduced ablation-front perturbations and enhanced thermal transport, both of which are critical for achieving high-performance fusion. Moreover, doping the ablator layer with these elements also helps mitigate the effects of high-Z impurities, which can strongly affect the hohlraum plasma conditions and degrade fusion performance.

Our calculations indicate that the introduction of a beryllium layer doped with sodium (Na) and bromine (Br) increases the maximum mass density by approximately 8.5%, thereby facilitating the formation of hot spots. Additionally, the implementation of a doped beryllium layer results in a 14% reduction in internal explosion speed, thereby effectively reducing the hydrodynamic instability of the shell during the implosion process. Moreover, the presence of a doped beryllium layer elevates the target gain from the break-even value ($G \approx 1$) to an approximate value of $G \approx 12$. Consequently, the use of a doped Be ablator layer offers the potential to enhance fusion performance, positioning it as a promising candidate for future inertial confinement fusion experiments. However, further research is imperative to optimize the doping level and other associated parameters to achieve even higher fusion yields. Additionally, additional experimental and theoretical investigations are warranted to comprehensively comprehend the underlying physics governing the improved ablator stability and its impact on the fusion process. Notwithstanding these considerations, our findings provide a robust foundation for future studies involving doped Be ablator layers in inertial confinement fusion, thereby opening up new avenues for advancing our understanding of high-energy-density physics.

Conflict of Interest

The authors declare no potential conflict of interest regarding the publication of this work.

References

Atzeni, S. and Meyer-ter Vehn, J. (2004). *The physics of inertial fusion: beam plasma interaction, hydrodynamics, hot dense matter*, volume 125. OUP Oxford.

Craxton, R., Anderson, K., Boehly, T., et al. (2015). Direct-drive inertial confinement fusion: A review. *Physics of Plasmas*, 22(11):110501.

Dittrich, T., Hurricane, O., Callahan, D., et al. (2014). Design of a high-foot high-adiabat ICF capsule for the National Ignition Facility. *Physical Review Letters*, 112(5):055002.

Haan, S., Amendt, P., Dittrich, T., et al. (2004). Design and simulations of indirect drive ignition targets for NIF. *Nuclear Fusion*, 44(12):S171.

He, X. and Zhang, W. (2007). Inertial fusion research in China. *The European Physical Journal D*, 44:227–231.

Hinkel, D., Hopkins, L. B., Ma, T., et al. (2016). Development of improved radiation drive environment for high foot implosions at the National Ignition Facility. *Physical Review letters*, 117(22):225002.

Huang, H., Xu, H., Youngblood, K., et al. (2012). Dopant Distribution in NIF Beryllium Ablator Capsules. In *APS Division of Plasma Physics Meeting Abstracts*, volume 54, pages GO4–012.

Kawata, S. (2021). Direct-drive heavy ion beam inertial confinement fusion: a review, toward our future energy source. *Advances in Physics: X*, 6(1):1873860.

Kline, J., Batha, S., Benedetti, L., et al. (2019). Progress of indirect drive inertial confinement fusion in the United States. *Nuclear Fusion*, 59(11):112018.

Kritcher, A., Clark, D., Haan, S., et al. (2018). Comparison of plastic, high density carbon, and beryllium as indirect drive NIF ablators. *Physics of Plasmas*, 25(5):056309.

Landen, O., Bradley, D., Braun, D., et al. (2008). Experimental studies of ICF indirect-drive Be and high density C candidate ablators. In *Journal of Physics: Conference Series*, volume 112, page 022004. IOP Publishing.

Lindl, J. (1995). Development of the indirect-drive approach to inertial confinement fusion and the target physics basis for ignition and gain. *Physics of Plasmas*, 2(11):3933–4024.

Lindl, J. D., Amendt, P., Berger, R. L., et al. (2004). The physics basis for ignition using indirect-drive targets on the National Ignition Facility. *Physics of Plasmas*, 11(2):339–491.

Lindl, J. D., McCrory, R. L., and Campbell, E. M. (1992). Progress toward ignition and burn propagation in inertial confinement fusion. *Phys. Today*, 45(9):32.

Logan, B. G., Perkins, L., and Barnard, J. (2008). Direct drive heavy-ion-beam inertial fusion at high coupling efficiency. *Physics of Plasmas*, 15(7):072701.

Loomis, E. N., Yi, S. A., Kyrala, G. A., et al. (2018). Implosion shape control of high-velocity, large case-to-capsule ratio beryllium ablators at the National Ignition Facility. *Physics of Plasmas*, 25(7):072708.

McClarren, R. G., Tregillis, I., Urbatsch, T. J., et al. (2021). High-energy density hohlraum design using forward and inverse deep neural networks. *Physics Letters A*, 396:127243.

McCrory, R., Meyerhofer, D., Betti, R., et al. (2008). Progress in direct-drive inertial confinement fusion. *Physics of Plasmas*, 15(5):055503.

McEachern, R. and Alford, C. (1999). Evaluation of boron-doped beryllium as an ablator for NIF target capsules. *Fusion Technology*, 35(2):115–118.

Murakami, M. and Meyer-ter Vehn, J. (1991). Indirectly driven targets for inertial confinement fusion. *Nuclear Fusion*, 31(7):1315.

Pfalzner, S. (2006). *An introduction to inertial confinement fusion*. CRC Press.

Ramis, R., Eidmann, K., Meyer-ter Vehn, J., et al. (2012). MULTI-fs–A computer code for laser–plasma interaction in the femtosecond regime. *Computer Physics Communications*, 183(3):637–655.

Ramis, R. and Meyer-ter Vehn, J. (2016). MULTI-IFEA one-dimensional computer code for Inertial Fusion Energy (IFE) target simulations. *Computer Physics Communications*, 203:226–237.

Ramis, R., Schmalz, R., and Meyer-ter Vehn, J. (1988). Multia computer code for one-dimensional multigroup radiation hydrodynamics. *Computer Physics Communications*, 49(3):475–505.

Rosen, M. D. (1999). The physics issues that determine inertial confinement fusion target gain and driver requirements: A tutorial. *Physics of Plasmas*, 6(5):1690–1699.

Slutz, S., Bailey, J., Chandler, G., et al. (2003). Dynamic hohlraum driven inertial fusion capsules. *Physics of Plasmas*, 10(5):1875–1882.

Tikhonchuk, V. (2020). Progress and opportunities for inertial fusion energy in Europe. *Philosophical Transactions of the Royal Society A*, 378(2184):20200013.

Yamanaka, C. (1999). Inertial confinement fusion: The quest for ignition and energy gain using indirect drive. *Nuclear Fusion*, 39(6):825–827.

Zylstra, A. B., Yi, S. A., MacLaren, S., et al. (2018). Beryllium capsule implosions at a case-to-capsule ratio of 3.7 on the National Ignition Facility. *Physics of Plasmas*, 25(10):102704.

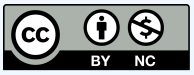

To cite this article:

Khanbabaei, B. (2023). Enhancing inertial confinement fusion with doped beryllium ablator layer in indirect drive scheme. *Radiation Physics and Engineering*, 4(4), 35-42.

DOI: 10.22034/rpe.2023.395904.1133

To link to this article: https://doi.org/10.22034/rpe.2023.395904.1133